

# ADVANCED WIDE AREA FAULT LOCATION AND CLASSIFICATION USING PHASOR MEASUREMENTS UNITS

**First A. Y. HATATA, Second M. M. EL-SAADAWI,**

Electric engineering Dept., Faculty of engineering, Mansoura university, Egypt,

**Third A. HELMY**

Electric engineering Dept., Faculty of engineering, Mansoura university, Egypt,  
eng\_ahmed\_helmy2010@yahoo.com

**Abstract:** Electric power systems are frequently subjected to different failures. The majority of these failures, i.e. faults, are related to transmission networks. In case of any fault, the faulty line should be isolated to overcome the hazards related to that fault and to minimize the damage impact on the faulty element. This action must be done as fast and accurate as possible.

This paper presents a proposed technique for wide area protection of power systems based on phasor measurement units. The proposed technique provides rapid, accurate, and reliable fault detection, classification, and location algorithms. Firstly, the technique detects the faulty line in the transmission networks, and then it classifies the faulty phase. Finally, it detects the fault location on the specified transmission line. The proposed algorithm is based on measuring both synchronized currents and voltages at transmission line terminals. The technique is tested on homogenous and non-homogenous single circuit and double circuit transmission lines of an IEEE-9 bus system. The simulations results prove the applicability and accuracy of the proposed technique.

**Key words:** phasor measurement unit (PMU), fault detection, fault classification, fault location, compound transmission networks, Wide area protection.

## 1. Introduction

Transmission networks are considered as the backbone of the power systems as they are responsible for continuity of service from generation stations to the end user customers. Overhead transmission lines and underground cables are subjected to faults on a daily basis. They need longer time to repair as operators take a lot of time to locate the faults. Due to economic and operational considerations, it is so important to minimize their outage times. Hence, a rapid and accurate fault detection, classification and location are so urgent and important tasks for power system operators [1–3].

Many techniques have been proposed in the past for estimating fault locations. The techniques, proposed in literature or implemented in practice, depended on using voltages and currents measured at one or both terminals of a line. These techniques can be divided into three categories: techniques based on travelling waves phenomenon, techniques based on

high-frequency components of currents and voltages generated by faults, and techniques based on fundamental-frequency currents and voltages measured at the terminals of a line [4].

In one-terminal fault location systems, the fault location devices are installed on one terminal of transmission lines, so that there are no communication devices are used. These methods are more economical than two-terminal fault location ones [5–11]. On other hand, these methods have low accuracy due to variations in loads, fault occurrence angles and both of source and fault impedances.

Development of new and effective means of communication between the line terminals has opened the opportunity for improving the fault location accuracy. Multi-terminal algorithms which use voltages, currents, or both of them synchronously or asynchronously have been developed. In these methods, the currents and voltages are measured from two terminals [12–14] or from multi terminals [15–16]. The multi-terminal methods are theoretically more accurate and less influenced by the fault resistance and remote terminal system's impedance. Nowadays, the multi-terminal algorithms can be executed easily due to the increase development of synchronized measurement elements based on Global Positioning System (GPS) comprising phasor measurement units (PMUs) [17]. Hence, the fault location techniques based on synchronized phasor measurements have rapidly become well-known techniques.

Several PMU-based fault location techniques have been proposed during the last decade. These techniques either use both synchronized current and voltage phasors data [18–23] or use only the synchronized voltage phasor data [24–26]. Although the methods depending on voltage data only are so simple, they may fail in case of faults with high resistances.

In this paper, a fast and efficient fault detection, classification, and location proposed technique is presented. The technique is based on synchronized measurements units for two-terminal compound

transmission lines. The technique depends on measuring the voltages and currents on both ends of the transmission line.

The paper is organized as follows. The synchronized PMU technology is presented in section 2. Wide area protection algorithm of power systems is presented in section 3. The evaluation of the proposed method and the results of the case studies are presented in section 4. Finally, the conclusion is presented in section 5.

## 2. Synchronized PMU technology

PMUs provide phasor measured data (both voltage and current magnitudes and phase angles) in the real times as shown in Fig. 1. Referring phase angle to a global reference time is useful in measuring the wide area snap shot of the power system [17].

PMUs have become the best measurement technology in electric power systems due to their minimal phase angle and frequency errors. They are become the essential devices for many applications in electric power systems. They supply synchronized positive sequence current and voltage measurements within a microsecond. They also used to measure the frequency and the rate of change of frequency (ROCOF). The satellite positioning (GPS) is currently the most common means of synchronization [17].

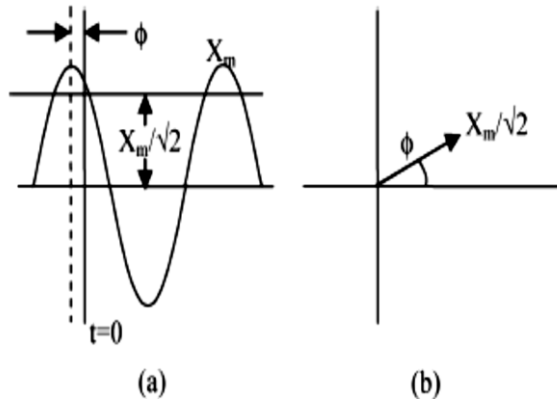


Fig. 1 Representation of a sinusoidal signal (a) Sinusoidal signal. (b) Phasor representation.

## 3. Wide area protection algorithm of power systems

This paper proposes a wide area protection scheme for power transmission lines. The proposed algorithm consists of three stages; fault detection, fault classification and fault location stages. The proposed algorithm is based on both current and voltage measurements. Figure 2 illustrates the flow chart of the proposed algorithm. The procedure of each stage will be explained in the following subsections.

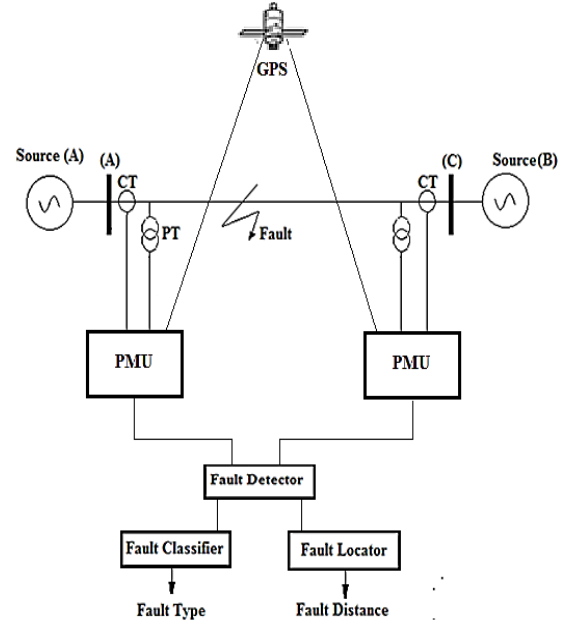


Fig. 2 Flow chart of the proposed algorithm

### 3.1 Fault detection stage

Once the fault takes place in any part of a power system, there will be significant disturbances in the system parameters: current, voltage, impedance, power, power factor, frequency, and power flow direction. The changes in these parameters will provide a good way to distinguish between abnormal and faulty conditions [27].

The proposed fault detection stage is based mainly on detecting the voltage magnitude reduction due to fault occurrence and comparing it permanently with a predefined value. Firstly, the positive sequence voltage magnitudes at each bus in the system are obtained and sorted by the PMUs. Then the collected voltages are compared with the initial buses voltages. This can lead to know the minimum voltage value which indicates the area to the fault. The minimum positive sequence voltage magnitude,  $V_{k\_min}^1$ , is determined and compared to its initial value,  $V_{k\_init}^1$  (where  $k \in [1: N]$  is the bus number). In case that the minimum voltage is lesser than the initial voltage value, there will be an indication of fault occurrence in the area of bus  $k$ . Otherwise; no fault will be recorded in that area.

To identify the faulty line, the absolute differences of the positive sequence current phase angles are collected by PMU units for all lines ( $M$ ) related to the faulty area bus. For a transmission line, connecting bus " $k$ " with bus " $j$ ", the absolute difference of positive sequence current angle is evaluated as:

$$\Delta\Phi_{kj} = |\Phi_k - \Phi_j| \quad (1)$$

The maximum absolute difference of positive sequence current angle results from the faulty line and hence it can be identified. The procedure of the proposed fault detection scheme is shown in Fig. 3.

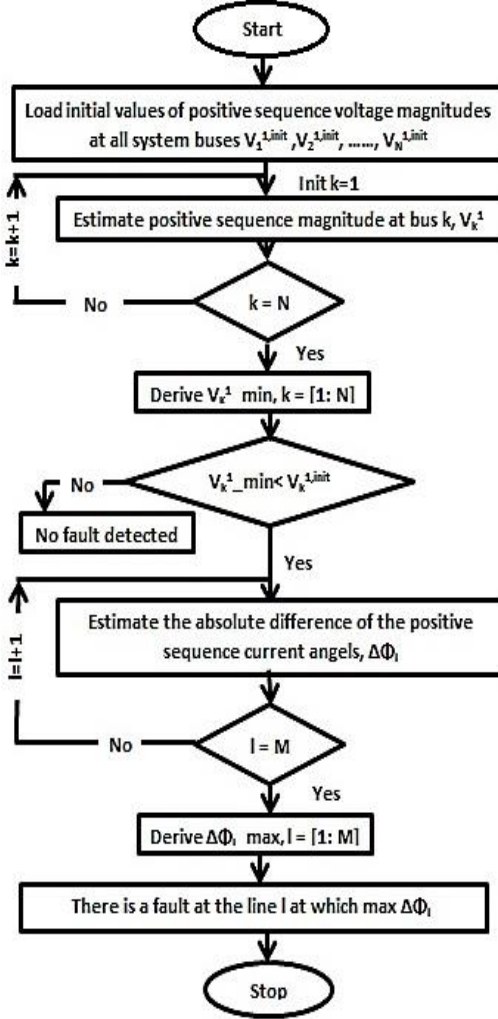


Fig. 3 Fault detection scheme

### 3.2 Fault classification stage

After detecting the fault, it is essential to identify the faulty phase and classify the fault type. This stage is very important to detect the next stage i.e. fault location on the faulty transmission lines. In practice, most of the faults occur on transmission networks are asymmetrical faults. The common types of asymmetric faults are single phase to ground, phase to phase and double phase to ground faults.

The fault is considered as a ground fault if the zero-sequence current,  $I_{zero}$  is greater than its pre-fault threshold value.  $I_{zero}$  can be obtained for fault classification as:

$$I_{zero} = \frac{I_a + I_b + I_c}{3} \quad (2)$$

The type of the specified fault is obtained by comparing the rate of change in all three phase

currents, i.e. ( $\Delta I_a$ ,  $\Delta I_b$ , and  $\Delta I_c$ ), with their predefined disturbance detection pickup values, i.e. ( $\Delta I_a^0$ ,  $\Delta I_b^0$ , and  $\Delta I_c^0$ ), which exactly leads to determine the faulty phase/phases. Figure 4 shows the procedure of the proposed fault classification scheme.

An integer variable  $P_i$  is defined to represent phases a, b, and c. The value of  $P_i$  will be one in case of there is a fault on this phase and or zero otherwise. Hence, the output of this stage will be a variable vector,  $P$ , where  $P = [P_a \ P_b \ P_c \ P_0]$  and  $P_0$  refers to ground fault.

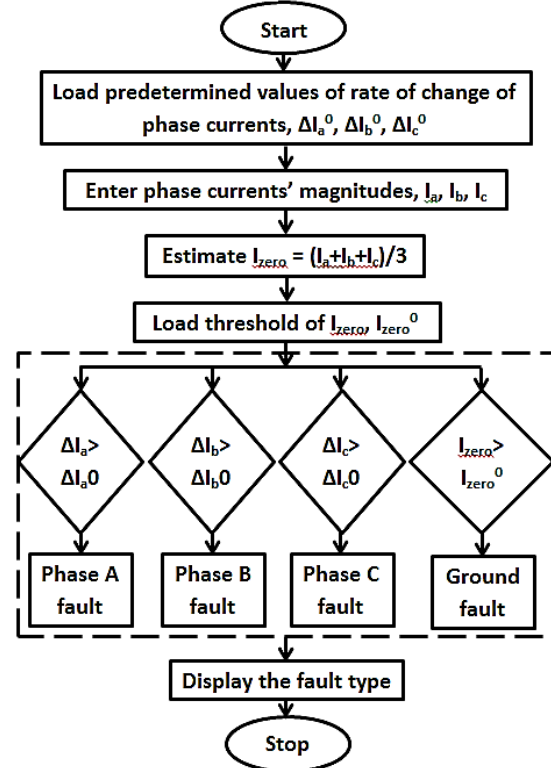


Fig. 4 Fault classification scheme

### 3.3 Fault location stage

This stage is used for the accurate determining of the fault location on the transmission line. It reduces the repairs times and operating costs by avoiding lengthy and expensive patrols. The following subsections will describe the fault location technique for different types of transmission systems.

#### A. Homogenous single circuit transmission line

For simplicity, we firstly apply the proposed algorithm to a single circuit homogeneous transmission line. A homogeneous transmission line is the line where impedance is distributed uniformly along its whole length. Figure 5 shows a single line diagram for a simple homogeneous two terminal transmission line, where bus S and R refer to sending and receiving end buses respectively [28–29].

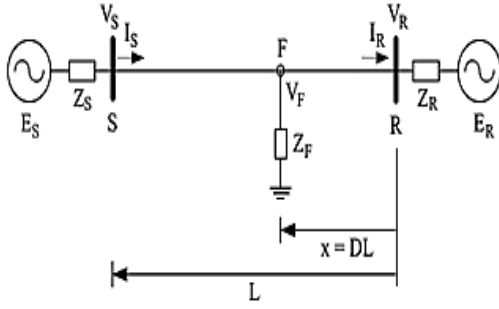


Fig. 5 Homogenous single circuit transmission line with a fault at a distance "x" from receiving end R.

The symmetrical components transformation method is used for analyzing of the three currents and voltages to three components. Also, it is used to consider the change of a distance variable (kilometers). The relation between the voltages and currents as a function of the distance away from bus R can be expressed by [30]:

$$\frac{\partial V_{012}}{\partial x} = Z_{012} * I_{012} \quad (3)$$

$$\frac{\partial I_{012}}{\partial x} = Y_{012} * V_{012} \quad (4)$$

where  $V_{012}$  and  $I_{012}$  are the voltage and current matrices represent the zero, positive, and negative-sequence components respectively.  $Z_{012}$  and  $Y_{012}$  denote the sequence impedance and admittance per unit of length of the transmission line, respectively. The matrices of  $Z_{012}$  and  $Y_{012}$  are diagonal matrices with diagonal entries of the zero, positive and negative sequence impedances ( $Z_0, Z_1, Z_2$ ) and admittance ( $Y_0, Y_1, Y_2$ ), respectively. The solutions of voltages and currents in (3) and (4) can be expressed as [1]:

$$V_{x1} = A_1 * e^{\gamma_1 * x} + B_1 * e^{-\gamma_1 * x} \quad (5)$$

$$I_{x1} = \frac{1}{Z_{c1}} * [A_1 * e^{\gamma_1 * x} - B_1 * e^{-\gamma_1 * x}] \quad (6)$$

where  $Z_c = \sqrt{Z/Y}$  is the characteristic impedance and  $\gamma = \sqrt{Z * Y}$  is the propagation constant. The constants  $A_1$  and  $B_1$  can be determined from the boundary conditions of voltages and currents measured at buses S and R, respectively. The receiving and sending end voltages in (5) can be rewritten as:

$$V_{x1,R} = \frac{V_{1,R} + Z_{c1} * I_{1,R}}{2} * e^{\gamma_1 * x} + \frac{V_{1,R} - Z_{c1} * I_{1,R}}{2} * e^{-\gamma_1 * x} \quad (7)$$

$$V_{x1,S} = e^{-\gamma_1 * L} * \frac{V_{1,S} + Z_{c1} * I_{1,S}}{2} * e^{\gamma_1 * x} + e^{\gamma_1 * L} * \frac{V_{1,S} - Z_{c1} * I_{1,S}}{2} * e^{-\gamma_1 * x} \quad (8)$$

Since the positive-sequence quantities are found in all fault types. So, they are used to compute the fault

locations in this paper. Equations (7) and (8) represent the positive voltages at point "x", which are expressed in terms of voltage and current at both receiving end ( $V_{1,R}, I_{1,R}$ ) and sending end ( $V_{1,S}, I_{1,S}$ ).

Now assume a fault occurred at point "F" at a distance " $x = D * L$ " from receiving end bus "R", where "L" is the transmission line length and "D" referred to the per-unit fault location index. Equalizing the voltage at point "F" measured from both ends S and R; i.e.  $V_{F,R} = V_{F,S}$  and solving for the index "D" we get [31-32]:

$$D = \frac{\ln(\frac{N}{M})}{2 * \gamma * L} \quad (9)$$

Where

$$M = \frac{1}{2} * ((V_S + Z_c * I_S) * e^{-\gamma * L} - (V_R + Z_c * I_R)) \quad (10)$$

$$N = \frac{1}{2} * ((V_R - Z_c * I_R) - (V_S - Z_c * I_S) * e^{\gamma * L}) \quad (11)$$

If the fault occurred within the protected line i.e. between bus S and R, then the value of D will be between 0 and 1. Otherwise; the value of D will be indefinite. From equations (9), (10), and (11) it is clear that, the variations in loading change, source impedance, inception angle and fault impedance, and type doesn't affect the value of the index "D".

### B. Non-homogenous single circuit transmission line

The overhead transmission lines combined with underground cables have been widely used in the modern cities. Such combination is called non-homogenous transmission lines. This section presents a proposed algorithm for faults location in non-homogenous transmission lines. Figure 6 shows a non-homogenous transmission line of length L composed of an overhead transmission line section of length  $L_S$  and an underground cable section of length  $L_R$ . PMUs are installed at both receiving and sending end buses.

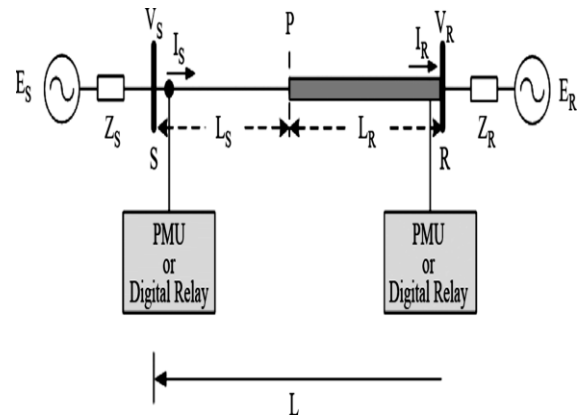


Fig. 6 Single line diagram of a two-section compound transmission line

The connection point between line section  $L_S$  and  $L_R$ , i.e. tap point P, can be represented as a theoretical receiving end for  $L_S$  and as a theoretical sending end of the cable. Because of the nature of combined lines, the non-uniform line impedance will be expected in this case.

The following procedure illustrates the proposed fault location technique:

Firstly, a fault in the underground cable section side,  $L_R$ , is assumed. In this case, the voltage and current at the point P can be obtained in terms of the sending end data sets ( $V_S$ ,  $I_S$ ) as:

$$V_{P,S} = \frac{1}{2} * (e^{-\gamma_S * L_S} * (V_S + Z_{c,S} * I_S) + e^{\gamma_S * L_S} * (V_S - Z_{c,S} * I_S)) \quad (12)$$

$$I_{P,S} = \frac{1}{2} * \frac{1}{Z_{c,S}} * (e^{-\gamma_S * L_S} * (V_S + Z_{c,S} * I_S) - e^{\gamma_S * L_S} * (V_S - Z_{c,S} * I_S)) \quad (13)$$

where  $Z_{c,S}$  and  $\gamma_S$  refer to the characteristic impedance and the propagation constants of the overhead line section respectively.

Since the voltage at any fault point in  $L_R$  section is the same when calculated in terms of sending end (i.e. tap point P) or receiving end (bus R). Then fault location index for this case can be obtained by substituting  $V_{P,S}$  and  $I_{P,S}$  into (8) and equating the result with (7) as follows [29]:

$$D_R = \frac{\ln(\frac{N_R}{M_R})}{2 * \gamma_R * L_R} \quad (14)$$

where

$$M_R = \frac{1}{2} * ((V_{P,S} + Z_{c,S} * I_{P,S}) * e^{-\gamma_R * L_R} - (V_R + Z_{c,R} * I_R)) \quad (15)$$

$$N_R = \frac{1}{2} * ((V_R - Z_{c,R} * I_R) - (V_{P,S} - Z_{c,S} * I_{P,S}) * e^{\gamma_R * L_R}) \quad (16)$$

where  $Z_{c,R}$  and  $\gamma_R$  refer to the characteristic impedance and the propagation constants of the underground cable section  $L_R$ , respectively.

In a similar manner, a fault on the overhead line section is assumed. In this case, the fault location index  $D_S$  can be obtained as follows:

$$D_S = \frac{\ln(\frac{N_S}{M_S})}{2 * \gamma_S * L_S} \quad (17)$$

where

$$M_S = \frac{1}{2} * ((V_S + Z_{c,S} * I_S) * e^{-\gamma_S * L_S} - (V_{P,R} + Z_{c,S} * I_{P,R})) \quad (18)$$

$$N_S = \frac{1}{2} * ((V_{P,R} - Z_{c,S} * I_{P,R}) - (V_S - Z_{c,S} * I_S) * e^{\gamma_S * L_S}) \quad (19)$$

Finally, faulty section should be identified exactly for any fault. The  $L_R$  section is chosen to be the

unified reference length for fault location, and its two terminals, i.e. tap point (P) and bus R, are the reference sending and receiving ends, respectively. From the previous discussion, both voltage angles and magnitudes at any point are the same when calculated from sending or receiving end. Figure 8 shows the curves of voltage magnitudes measured at buses S and R for a fault at point F on the  $L_S$  section of the transmission line.

As shown in Figure 7, the slope of  $|V_R|$  is not the same in both right hand and left hand sides of the tap point, P, this is due to the non-similarity of the line impedances of  $L_R$  and  $L_S$  sections. Both of the voltage curves seem to decrease linearly and pointing to the fault position [14]. The amplitude of the fault voltage  $V_F$  is the intersection point of the voltage curves.

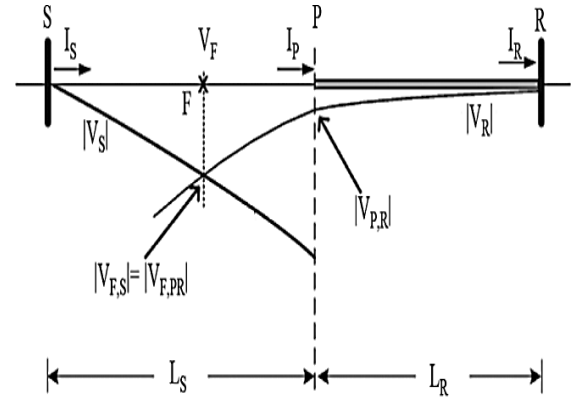


Fig. 7 Relation between  $|V_S|$  and  $|V_R|$  curves for fault F on  $L_S$  section

As  $|V_{F,PR}| = |V_{F,PS}|$ , the index  $D_S$  can be obtained as mentioned previously. Since  $D_S$  is calculated by assuming  $L_S$  as the reference length and its two terminals, i.e. S and P, as the reference sending and receiving ends, respectively, the obtained  $D_S$  will be in the interval  $[0, 1]$ . Furthermore, there will not be intersections of  $|V_S|$  and  $|V_R|$  in  $L_R$  section, which lead to that  $D_R$  may not converge in interval  $[0, 1]$ .

By the same technique, both  $D_S$  and  $D_R$  and their relationships can be deduced for faults on underground cable section  $L_R$  or at tap point, P. The resulting relationships can be summarized as:

- 1) If  $D_S < 0$  and  $0 \leq D_R < 1$  then the fault is in  $L_R$  section and its location is  $D_R$  from bus R.
- 2) If  $0 \leq D_S < 1$  and  $D_R > 1$  then the fault is in  $L_S$  section and its location is  $(1 - D_S)$  from bus S.
- 3) If  $D_S = 0$  and  $D_R = 1$  then the fault is at tap point P.

A Flowchart outlines the proposed fault location algorithm is shown in Figure 8.

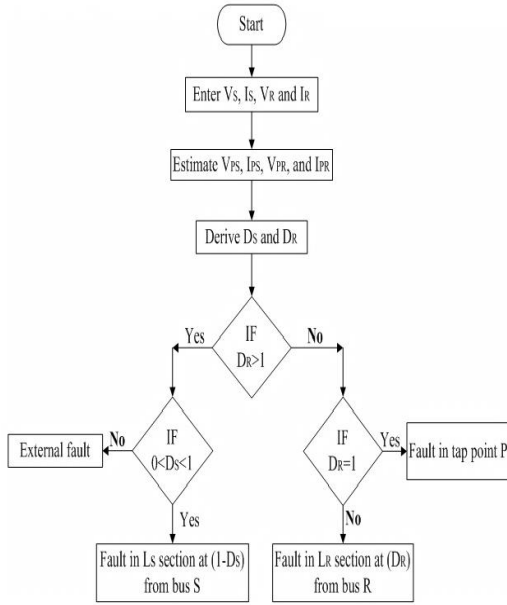


Fig. 8 Flowchart of the proposed fault location algorithm

#### C. Double circuit transmission line

The double circuit transmission line system is widely-used in transmission network due to its reliability and economic reasons. It can be considered as two independent lines, as only positive sequence data is used to identify the measured values in the proposed algorithm. Figure 9 demonstrates a double circuit transmission line system, which is equivalent to two individual non-homogenous single circuit transmission lines.

When a fault occurs in a line, the current at both sides of that line are in different direction. This phenomenon can be used to determine the faulty line. After detecting the faulty line, the proposed fault location technique can directly be applied on that line.

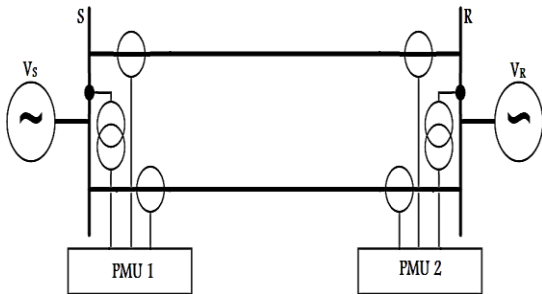


Fig. 9 Double circuit transmission line system

#### 4. Performance evaluation

The proposed algorithm is developed in MATLAB® environment. Then it is applied to two test systems; a simple double circuit non-homogenous transmission line and an IEEE 9-bus system.

#### 4.1 Double circuit non-homogenous transmission line

In this case, the proposed algorithms are applied to a test system consists of a transposed double-circuit two-terminal two-section non-homogeneous line with zero sequence mutual coupling system as shown in Fig. 10.

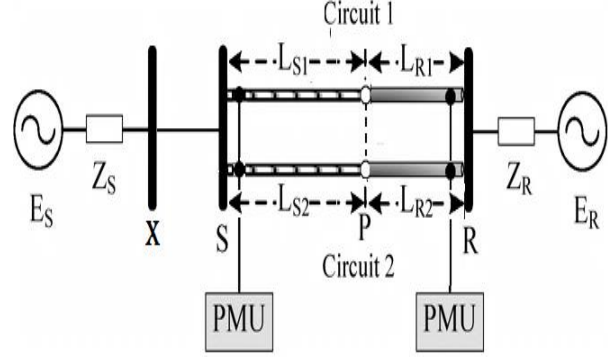


Fig. 10 Single line diagram of double-circuit two-section transmission system

Line X-S is used to examine external faults. The system is simulated in MATLAB/SIMULINK® environment and the system parameters are summarized in Table I. The system is simulated under different system operation and fault conditions. The percentage error of fault location estimation is evaluated as:

$$\text{Error \%} = \frac{|\text{Estimated location} - \text{Real location}|}{\text{Total length of T.Line}} * 100\% \quad (20)$$

The proposed fault location algorithm is applied to the test system, for different fault types and at different fault locations. All measurements are sampled due to a sampling frequency of 4000 Hz (80 sample per cycle). Hereafter, the results of some selected cases are presented in details.

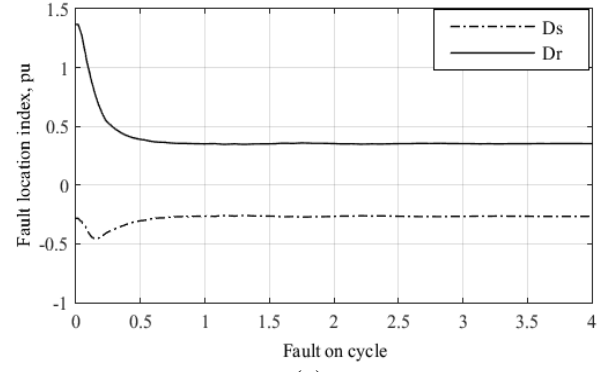
1. *Three phase to ground fault:* The fault occurs in the first circuit at line  $L_R$  (internal fault) at distance 35 Km away from bus R (35% of line length) with fault resistance,  $R_f = 10 \Omega$  and the fault inception angle is zero degree with respect to phase 'a' voltage waveform at bus S. Figure (11-a) shows the fault location indices  $D_R$  and  $D_S$ , it can be noticed that they are converged with  $D_R$  between [0, 1]. Then, according to fault location algorithm,  $D_R = 0.3527$  p.u is the suitable fault index choose, with error 0.14%.
2. *Phase to phase fault (B-C fault):* The fault occurs in the second circuit at line  $L_S$  at distance 45 Km away from bus S (50% of line length) with  $R_f = 0.1 \Omega$ . Figure (11-b) shows fault location indices  $D_R$

and  $D_S$ , it can be noticed that both  $D_R$  and  $D_S$  converged. While  $D_S = 0.5033$  p.u ( $\in [0, 1]$ ) is the correct index with error 0.156%.

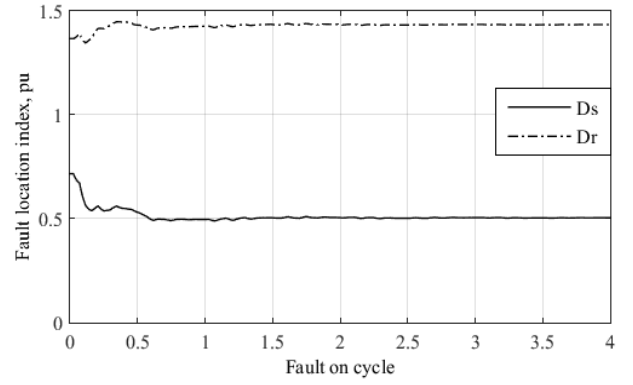
3. *Fault at tap point*: In this case, the fault indices values are:  $D_R=1.0144$  p.u and  $D_S=0.0272$  p.u. Figure (11-c) shows the response for this fault.
4. *Phase to ground fault (A-g fault)*: The fault occurs in line  $X_S$  at a distance of 50 Km from bus S “external fault”. It is observed that both  $D_S$  and  $D_R$  don’t converge between  $[0, 1]$ , as shown in figure (11-d).

Table 1  
Parameters of 220 KV Double Circuit Two Terminal Nonhomogeneous Transmission Line System

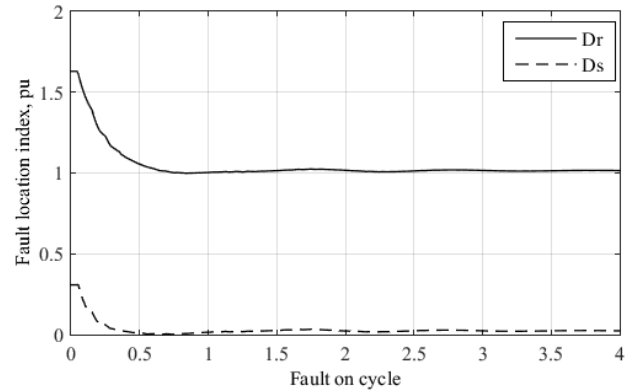
System voltage		220 KV	
frequency		50 Hz	
$E_S=$	$1\angle 10^\circ$	$Z_{S1}=$	$0.24+j5.72 \Omega$
$E_R=$	$1\angle 0^\circ$	$Z_{R1}=$	$0.24+j5.72 \Omega$
$L_R=$	100Km	$Z_{S0}=$	$2.74+j10 \Omega$
$L_S=$	90 Km	$Z_{R0}=$	$2.74+j10 \Omega$
$L_X=$	200Km		
Positive sequence			
$R_{1\_LR}=$	0.016 $\Omega$ /Km	$L_{1\_LR}=$	0.268 mH/Km
$R_{1\_LS}=$	0.024 $\Omega$ /Km	$L_{1\_LS}=$	0.256 mH/Km
$R_{1\_LX}=$	0.0058 $\Omega$ /Km	$L_{1\_LX}=$	0.6341 mH/Km
$C_{1\_LR}=$	456.9 nF/Km		
$C_{1\_LS}=$	457.63nF/Km		
$C_{1\_LX}=$	18.4 nF/Km		
Zero sequence			
$R_{0\_LR}=$	0.059 $\Omega$ /Km	$L_{0\_LR}=$	0.206 mH/Km
$R_{0\_LS}=$	0.036 $\Omega$ /Km	$L_{0\_LS}=$	0.332 mH/Km
$R_{0\_LX}=$	0.1067 $\Omega$ /Km	$L_{0\_LX}=$	2.2343 mH/Km
$C_{0\_LR}=$	456.9 nF/Km		
$C_{0\_LS}=$	457.63nF/Km		
$C_{0\_LX}=$	8.7 nF/Km		
Zero sequence mutual coupling			
$R_{0m\_LR}=$	0.004 $\Omega$ /Km	$L_{0m\_LR}=$	0.015 mH/Km
$R_{0m\_LS}=$	0.03 $\Omega$ /Km	$L_{0m\_LS}=$	0.011 mH/Km
$R_{0m\_LX}=$	1.0035 $\Omega$ /Km	$L_{0m\_LX}=$	1.2907 mH/Km
$C_{0m\_LR}=$	-1.427 nF/Km		
$C_{0m\_LS}=$	-3.077 nF/Km		
$C_{0m\_LX}=$	-3.4 nF/Km		



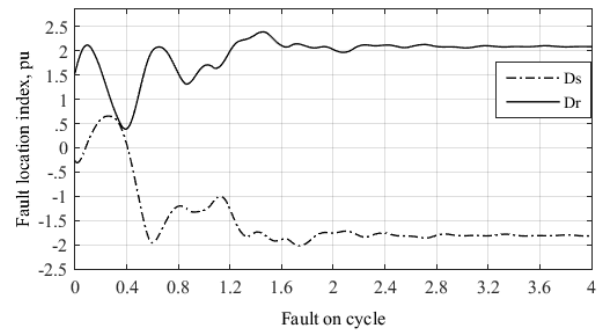
(a)



(b)



(c)



(d)

Fig. 11 Fault response curves for fault on (a)  $L_R$  in the 1<sup>st</sup> circuit, (b)  $L_S$  in the 2<sup>nd</sup> circuit, (c) tap point, and (d)  $X_S$  (external fault)



The developed program is applied to many cases for internal and external faults. These cases include ten different fault type [phase to ground, phase to phase, double to ground and three phase faults], three different fault resistance [ $0.1\Omega$ ,  $10\Omega$ , and  $1k\Omega$ ], three different fault inception angle [ $0^\circ$ ,  $30^\circ$ , and  $90^\circ$ ], and two different source impedances, at three different locations indices [10%, 50%, 90%]. The total number of these cases is 2880 case as illustrated by column 3 in Table 2. It can be easily shown that the implementation of the fault location algorithm under different fault conditions such as different fault types, fault resistances, fault inception angles, and source impedances, has excellent results with slightly errors with an average of 0.2451 %. To verify the accuracy of the proposed algorithm, the results have compared with those obtained in [26]. In that study, the method was applied to locate different types of faults using the synchronized voltage phasor data only. A comparison between the two methods is depicted in Tables II. It can be noticed that the proposed method is more accurate than that applied in [26].

Table 2

Sample Cases of the Tested Double Circuit Two Terminal Nonhomogeneous Transmission Line System

Actual fault location			Fault locations errors (%) proposed method		Fault locations errors (%) [24]	
Fault section	Fault position (% of line length)		Max.	Avg.	Max.	Avg.
$L_{R1}$	10%	from bus	0.3119	0.2356	0.452	0.263
	50%	bus	0.2531	0.1912	0.324	0.225
	90%	R	0.2901	0.2204	0.473	0.423
$L_{S1}$	10%	from bus	0.3524	0.2683	0.362	0.264
	50%	bus	0.3011	0.2305	0.302	0.224
	90%	S	0.3732	0.2837	0.325	0.298
$L_{R2}$	10%	from bus	0.3395	0.2527	0.336	0.246
	50%	bus	0.2725	0.2124	0.259	0.2013
	90%	R	0.3124	0.2333	0.310	0.235
$L_{S2}$	10%	from bus	0.3832	0.2879	0.386	0.279
	50%	bus	0.3312	0.2549	0.351	0.276
	90%	S	0.3903	0.2925	0.426	0.317
Tap point, P			0.3413	0.2235	0.356	0.245
External fault	10%	from bus	infinite number	-	-	-
	50%	bus	infinite number	-	-	-
	90%	S	infinite number	-	-	-

#### 4.2 IEEE 9-bus system

The proposed algorithm is applied to a modified IEEE 9-bus system. The test system is shown in Fig. 12. In this system, the branch from bus 7 to bus 8 is set as a nonhomogeneous section.

A three-phase fault is assumed in  $L_R$  section of line 6 at distance 40 Km away from bus 8 (40% of line length) with fault resistance,  $R_f=100\Omega$  and the fault inception angle is zero degree with respect to phase 'a' voltage waveform at bus 7.

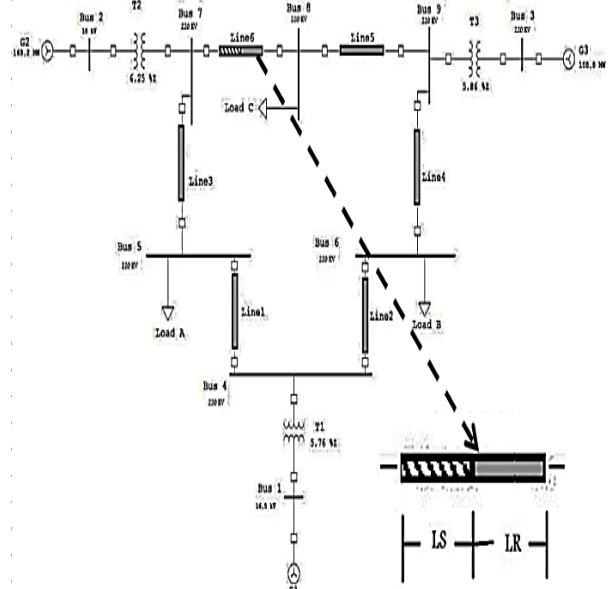


Fig. 12 Single line diagram of modified IEEE 9-bus system

Figure 13 shows the reduction of positive sequence voltage magnitudes measured by PMUs at each bus due to fault occurrence. It can be noticed that bus 8 has the minimum value of voltage magnitude. Comparing this value with a preset initial value, we find that  $V_8^1 < V_8^{1,init}$ , which means that there's a fault in the area of bus 8, i.e. line 5 or line 6.

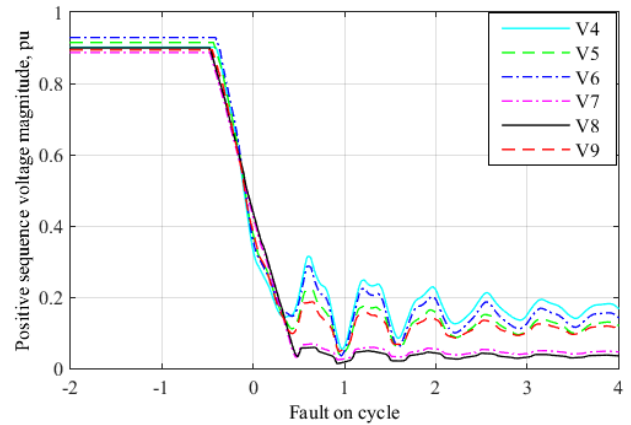


Fig. 13 Voltage magnitude at each bus in IEEE 9-bus system during the fault on line 6

Figure 14, illustrates the absolute differences of the positive sequence current angles for lines 5 and line 6, from which it can be noticed that the maximum absolute difference in angles is obtained for line 6, which mean that it is the faulted line.



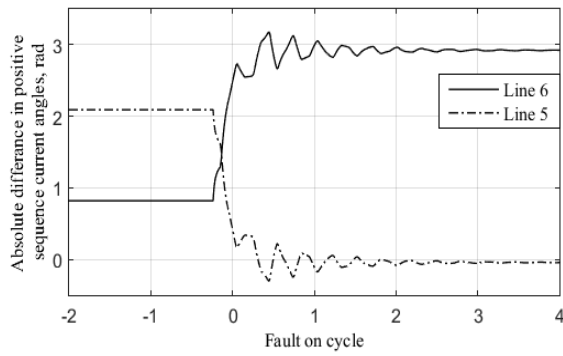


Fig. 14 Absolute differences for positive sequence current angles for lines (5 & 6) (i.e. bus 8 area)

To classify the fault, the proposed fault classification algorithm is applied. The resultant vector is,  $F = [1 \ 1 \ 1 \ 0]$  which indicates that there is a fault in all phases and while there is no ground fault, i.e. three phase fault.

Finally, applying fault location technique, it is found that the fault location index,  $D_R = 0.4028$  which locate the fault with accuracy 99.8674 %.

## 5. Conclusion

Advanced wide area fault detection, classification and location algorithms based on PMUs were proposed in this paper. All the three algorithms were modeled and simulated. For this purpose, a MATLAB codes were built and applied to different case studied. The proposed algorithms were applied to homogenous and non-homogenous transmission systems including single and double circuit transmission circuits. The proposed algorithm was tested on a modified IEEE 9-bus system. The simulation results prove that the performance of the proposed algorithm unaffected by system operation conditions, hence it is appropriate for all fault conditions. The overall simulation case studies show that the performance of the proposed algorithms is very excellent with accuracy exceeds 99%.

## Appendix

Table III  
Parameters of IEEE 9-Bus 220 KV System

$G_1$	$E_1=16.5 \text{ KV}, \theta_1=0^\circ, Z_{G1\_1}=0.238+j5.72 \text{ } (\Omega)$ $Z_{G1\_0}=2.738+j10 \text{ } (\Omega)$
$G_2$	$E_2=18.0 \text{ KV}, \theta_2=10^\circ, Z_{G2\_1}=0.238+j5.72 \text{ } (\Omega)$ $Z_{G2\_0}=2.738+j10 \text{ } (\Omega)$
$G_3$	$E_3=13.8 \text{ KV}, \theta_3=5^\circ, Z_{G3\_1}=0.238+j5.72 \text{ } (\Omega)$ $Z_{G3\_0}=2.738+j10 \text{ } (\Omega)$
$T_1$	100 MVA, 16.5/220 KV, $Z\%=5.76$
$T_2$	100 MVA, 18.0/220 KV, $Z\%=6.25$
$T_3$	100 MVA, 13.8/220 KV, $Z\%=5.86$
$L_A$	125 MW, 50 MVAR
$L_B$	90 MW, 30 MVAR
$L_C$	100 MW, 35 MVAR
$T.L_1$	$L_1=100 \text{ Km}, [r_1 \ r_0]=[0.0529 \ 0.13225] \Omega/\text{Km}$ $[l_1 \ l_0]=[1.192e-3 \ 2.38e-3] \text{ H/Km},$ $[c_1 \ c_0]=[8.82e-9 \ 5.188e-9] \text{ F/Km}$

$T.L_2$	$L_2=100 \text{ Km}, [r_1 \ r_0]=[0.0899 \ 0.22483] \Omega/\text{Km}$ $[l_1 \ l_0]=[1.29e-3 \ 3.22e-3] \text{ H/Km}$ $[c_1 \ c_0]=[7.922e-9 \ 4.74e-9] \text{ F/Km}$
$T.L_3$	$L_3=100 \text{ Km}, [r_1 \ r_0]=[0.16928 \ 0.4232] \Omega/\text{Km}$ $[l_1 \ l_0]=[2.259e-3 \ 5.64e-3] \text{ H/Km}$ $[c_1 \ c_0]=[15.34e-9 \ 9.025e-9] \text{ F/Km}$
$T.L_4$	$L_4=100 \text{ Km}, [r_1 \ r_0]=[0.20631 \ 0.5157] \Omega/\text{Km}$ $[l_1 \ l_0]=[2.38e-3 \ 6.09e-3] \text{ H/Km}$ $[c_1 \ c_0]=[17.95e-9 \ 10.55e-9] \text{ F/Km}$
$T.L_5$	$L_5=100 \text{ Km}, [r_1 \ r_0]=[0.0629 \ 0.15737] \Omega/\text{Km}$ $[l_1 \ l_0]=[1.414e-3 \ 3.53e-3] \text{ H/Km}$ $[c_1 \ c_0]=[10.47e-9 \ 6.15e-9] \text{ F/Km}$
$T.L_6$ ( $L_S$ )	$L_S=50 \text{ Km}, [r_1 \ r_0]=[0.04497 \ 0.11241] \Omega/\text{Km}$ $[l_1 \ l_0]=[1.01e-3 \ 2.02e-3] \text{ H/Km}$ $[c_1 \ c_0]=[7.471e-9 \ 4.39e-9] \text{ F/Km}$
$T.L_6$ ( $L_R$ )	$L_R=50 \text{ Km}, [r_1 \ r_0]=[0.016 \ 0.059] \Omega/\text{Km}$ $[l_1 \ l_0]=[2.68e-3 \ 2.06e-3] \text{ H/Km},$ $[c_1 \ c_0]=[18.45e-9 \ 8.75e-9] \text{ F/Km}$

## References

1. Saha, M.M., Izykowski J., Rosolowski, E. : *Fault Location on Power Networks*, Springer, 2009.
2. Guzman, A., Mooney, J.B., Benmouyal, G., Fischer, N. : *Transmission Line Protection System for Increasing Power System Requirements*. 55<sup>th</sup> Annual Conference for Protective Relay Engineers, College Station, Texas, April 2002.
3. Kezunovic, M. : *Intelligent Systems in Protection Engineering*. Power System Technology, Proceedings of PowerCon. 2000, 4-7 Dec. 2000, vol. 2, pp. 801-806.
4. Saha, M.M., Vero. Ratan P., Novosel, D., : *Review of Fault Location Techniques for Distribution Systems*. Power Systems and Communications Infrastructures for the future, Beijing, September 2002.
5. Liao, Y. : *Fault location for single-circuit line based on bus-impedance matrix utilizing voltage measurements*. IEEE Trans. Power Del., Vol .23, No. 2, Apr. 2008, pp. 609–617.
6. Ye, L., You, D., Yin, X., Wang, K., Wu., J. : *An improved fault-location method for distribution system using wavelets and support vector regression*. International Journal of Electrical Power & Energy Systems, Vol. 55, February 2014, pp. 467-472.
7. Takagi, T.T., Yamakoshi, Y., Baba, Baba, J., Uemura, K., Sakaguchi, T. : *Development of a new fault locator using the one-terminal voltage and current data*. IEEE Trans. Power App. Syst., vol. PAS-101, Aug. 1982, pp.2892–2898.
8. Eisa, A.A., Ramar, K. : *Accurate one-end fault location for overhead transmission lines in interconnected power systems*. Int. Electrical Power and Energy Systems, vol. 32, 2010, pp.383 – 389.
9. Guobing, S., Jiale, S., Yaozhong, G. : *An accurate fault location algorithm for parallel transmission lines using one-terminal data*. Int. Electrical Power and Energy Systems, Vol. 31, 2009, pp.124 – 129.

10. Ngu, E.E., Ramar, K., Eisa, A., : *One-end fault location method for untransposed four-circuit transmission lines*. Int. Electrical Power and Energy Systems, Vol. 43, 2012, pp.660 – 669.
11. Yerekar, S.R. : *Fault Location System for Transmission Lines in One-terminal By using Impedance-Traveling Wave Assembled Algorithm*. 8<sup>th</sup> EEIC international conference on environment and electrical engineering, Karpacz, Poland, May 10-13, 2009.
12. Novosel, D., Hart, D.G., Udren, E., Garitty, J. : *Unsynchronized two-terminal fault location estimation*. IEEE Trans. Power Del., Vol. 11, No. 1, Jan. 1996, pp. 130–138.
13. Silveira, E.G., Pereira, C. : *Transmission line fault location using two-terminal data without time synchronization*. IEEE Trans. Power Del., Vol. 22, No. 1, Feb. 2007, pp. 498–499.
14. Dalcastagnê, A.L., Filho, S.N., Zürn, H.H., and Seara, R. : *An iterative two-terminal fault-location method based on unsynchronized phasors*, IEEE Trans. Power Del., Vol. 23, No. 4, Oct. 2008, pp. 2318–2329.
15. Girgis, A.A., Hart, D.G., and Peterson, W.L. : *A new fault location technique for two-and three-terminal lines*, IEEE Trans. Power Del., Vol. 7, No. 1, Jan. 1992, pp. 98–107.
16. Lin, Y.H., Liu, C.W. and Yu, C.S. : *A new fault locator for three-terminal transmission lines Using two-terminal synchronized voltage and current phasors*, IEEE Trans. Power Del., Vol. 17, No. 2, Apr. 2004, pp.452–459.
17. Phdke, A.G. and Thorp, J.S. : *A text book of (Synchronized Phasor Measurements and Their Applications)*, Berlin, Germany, Springer, 2008.
18. Lien, K., Liu, C., Yu, C. and Jiang, J. : *Transmission network fault location observability with minimal PMU placement*, IEEE Transactions on Power Del., Vol. 21, No. 3, 2006, pp.1128–1136.
19. Shiroei, M., Daniar, S. and Akhbari, M. : *A new algorithm for fault location on transmission lines*, IEEE Power & Energy Society General Meeting, 2009, pp.1–5.
20. Wu, T., Li, J., Kamwa, I., Chung, C.Y., and Qin, M. : *A Synchrophasor Measurements-Based Fault Location Technique for Multi-terminal Multi-section Nonhomogeneous Transmission Lines*, IET Generation Transmission & Distribution, Vol.10, No. 8, 2016.
21. Lin, T.C., Lin, P.Y., and Liu, C.W. : *An Algorithm for Locating Faults in Three-Terminal Multisection Nonhomogeneous Transmission Lines Using Synchrophasor Measurements*, IEEE Trans. on Smart Grid, 2014.
22. Jiang, Q., Wang, B., and Li, X. : *An Efficient PMU-Based Fault-Location Technique for Multiterminal Transmission Lines*, IEEE Trans on Power Del., 2014.
23. Feng, G., and Ali A. : *Fault Location Using Wide-Area Measurements and Sparse Estimation*, IEEE Transactions on Power Systems, 2015.
24. Wang, C., Dou, C., Li, X., and Jia, Q. : *A WAMS/PMU-based fault location technique*, Electric Power Systems Research, Vol. 77, No. (8), 2007, pp. 936–945.
25. Firouzbah, K., and Sheikholeslami, A. : *A current independent method based on synchronized voltage measurement for fault location on transmission lines*, Simulation Modeling Practice and Theory, Vol. 17 No. 4, 2009, pp. 692–707
26. Jiang, Q., Li, X., Wang, B. and Wang, H. : *PMU-Based Fault Location Using Voltage Measurements in Large Transmission Networks*, IEEE Trans. Power Del., Vol. 27, No. 3, July 2012.
27. Blackburn, J.L. and Domin, T.J. : *Text book of Protective Relaying, Principles and Applications*, third edition, 2007.
28. Liu, C.W., Lien, K.P., Chen, C.S. and Jiang, J.A. : *A universal fault location technique for N-terminal [ $N \geq 3$ ] transmission lines*, IEEE Trans. Power Del., Vol. 23, No. 3, Jul. 2008, pp. 1366–1373.
29. Liu, C.W., Lin, T.C., Yu, C.S. and Yang, J.Z. : *A Fault Location Technique for Two-Terminal Multisection Compound Transmission Lines Using Synchronized Phasor Measurements*, IEEE Tran. on Smart Grid, Vol. 3, No. 1, March 2012.
30. Gross, C.A. : *Power System Analysis*. New York: Wiley, 1986.
31. Lin, Y.H., Liu, C.W. and Chen, C.S. : *An adaptive PMU based fault detection/location technique for transmission lines with consideration of arcing fault discrimination part I: Theory and algorithms*, IEEE Trans. Power Del., Vol. 19, No. 4, Oct. 2004, pp. 1587–1593.
32. Lin, Y.H., Liu, C.W. and Chen, C.S. : *An adaptive PMU based fault detection/location technique for transmission lines with consideration of arcing fault discrimination, part II: Performance evaluation*, IEEE Trans. Power Del., Vol. 19, No. 4, Oct. 2004, pp. 1594–1601.